

# Novel Molecular Organotin Oxides Derived from Alkylidene Bridged Ditin Precursors: Syntheses and Structures<sup>†,‡</sup>

Bernhard Zobel, Markus Schürmann, and Klaus Jurkschat\*

*Lehrstuhl für Anorganische Chemie II der Universität Dortmund,  
D-44221 Dortmund, Germany*

Dainis Dakternieks\* and Andrew Duthie

*School of Biological and Chemical Sciences, Deakin University, Geelong,  
Victoria 3217, Australia*

Received May 11, 1998

New diorganotin compounds  $(RCl_2Sn)_2(CR'_2)_n$  [ $R = (SiMe_3)_2CH$ ;  $R' = Me, H; n = 1-3$ ] linked by various spacers have been synthesized. These react with sodium hydroxide or  $(t-Bu_2SnO)_3$  to give  $(R(O)Sn)_2(CR'_2)_n$ . Compounds **8** ( $R' = Me, n = 1$ ), **9** ( $R' = H, n = 2$ ), and **10** ( $R' = H, n = 3$ ) contain four-coordinate tin atoms. Compound **9** undergoes a reversible hydrolysis reaction from which a solid containing three ditin units has been isolated. Evidence is presented for the existence in solution of monomeric four-coordinate tin compounds  $(RXSn)_2(CH_2)_3O$  [ $R = (SiMe_3)_2CH, X = Cl, OH$ ]. Crystal structures for monomeric ditin precursors 2,2-bis[bis(trimethylsilyl)methyldichlorostannyl]propane (**3**) and 1,2-bis[bis(trimethylsilyl)methyldichlorostannyl]ethane (**6**), for dimeric units 1,3,5,7-tetrakis[bis(trimethylsilyl)methyl]-9,9,10,10-tetramethyl-2,4,6,8-tetraoxa-1,3,5,7-tetrastadtannaadamantane (**8**), 1,3,7,9-tetrakis[bis(trimethylsilyl)methyl]-2,8,13,14-tetraoxatricyclo[7.3.1.13.7]-1,3,7,9-tetrastannatetradecane (**10**), and 2,6-difluoro-2,6-bis[bis(trimethylsilyl)methyl]-1-oxa-2,6-distannacyclohexane dimer (**12**), and for trimeric units  $\{O(RSn(CH_2)_2SnR)OH\}_3 \cdot 2H_2O$  (**9a**) are reported.

## Introduction

The structure and, hence, the properties of diorganotin oxides  $(R_2SnO)_n$  essentially depend on the nature of the organic substituent R. Insoluble polymers ( $n = \infty$ )<sup>1</sup> are observed for sterically nondemanding R groups such as Me, Et, n-Bu, or Ph as a result of intramolecular cross-linking<sup>2</sup> brought about by Sn–O Lewis acid–base interactions. Bulky substituents such as bis(trimethylsilyl)methyl, tris(trimethylsilyl)methyl, *tert*-butyl, *tert*-amyl, 2,6-diethylphenyl, 2,4,6-trimethylphenyl, or 2,4,6-tris(trifluoromethyl)phenyl inhibit cross-linking, and, consequently, well-defined molecular organotin oxides are formed, such as  $\{(Me_3Si)_2CH_2SnO\}_2$ ,<sup>3a</sup>  $\{(Me_3Si)_2CH(Me)Sn(OSn(Me)C(SiMe_3)_3)_2O\}$ ,<sup>3b</sup>  $(t-Bu_2SnO)_3$ ,<sup>3c</sup>  $[(t-C_5H_{11})_2SnO]_3$ ,<sup>3c</sup>  $[(2,6-Et_2C_6H_3)_2SnO]_3$ ,<sup>3d</sup>  $[(2,4,6-Me_3C_6H_2)_2SnO]_3$ ,<sup>3e</sup> and  $\{[2,4,6-(CF_3)_3C_6H_2]_2SnO\}_3$ .<sup>3f</sup>

<sup>†</sup> Dedicated to Professor R. R. Holmes on the occasion of his 70th birthday.

<sup>‡</sup>This paper includes part of the Ph.D. thesis of B. Zobel, Dortmund University, 1997.

(1) Harrison, P. G., Ed. *Chemistry of Tin*; Blackie & Son: London, 1983.

(2) Harris, R. K.; Sebald, A. J. *Organomet. Chem.* **1987**, *331*, C9.

(3) (a) Edelman, M. A.; Hitchcock, P. B.; Lappert, M. F. *J. Chem. Soc., Chem. Commun.* **1990**, 1116. (b) Belsky, K. K.; Zemlyansky, N. N.; Borisova, I. V.; Kolosova, N. D.; Beletskaya, I. P. *J. Organomet. Chem.* **1983**, *254*, 189. (c) Puff, H.; Schuh, W.; Sievers, R.; Wald, W.; Zimmer, R. *J. Organomet. Chem.* **1984**, *260*, 271. (d) Masamune, S.; Sita, C. R.; Williams, D. J. *J. Am. Chem. Soc.* **1983**, *105*, 630. (e) Weber, U.; Pauls, N.; Winter, W.; Stegmann, H. B. *Z. Naturforsch., B* **1982**, *37*, 1316. (f) Grützmacher, H.; Pritzkow, H. *Chem. Ber.* **1993**, *126*, 2409.

We have been interested for some time in bridged ditin compounds containing various spacers,  $(RCl_2Sn)-(CH_2)_n$  ( $R = Me_3SiCH_2, Ph; n = 1-4$ ).<sup>4</sup> On reaction with sulfide, selenide, or telluride, these derivatives provided well-defined molecular organotin chalcogenides with adamantane-type and tricyclic ring structures.<sup>4b,5</sup>

Reaction of  $[Me_3SiCH_2(Cl_2Sn)]_2(CH_2)_3$  with  $(t-Bu_2SnO)_3$  or with  $^{1/2}n\{[Me_3SiCH_2(O)Sn]_2(CH_2)_3\}_n$  gave  $\{[Me_3SiCH_2(Cl)Sn(CH_2)_3Sn(Cl)CH_2SiMe_3]O\}_4$ , the first tetraorganodistannoxane with a double ladder structure of type **A**<sup>4c,6</sup> (see Chart 1). It is interesting to note that alternative ditin and tetratin structures of types **B** and **C** were not observed.

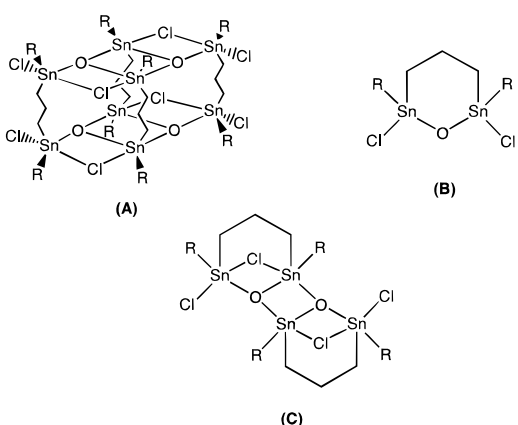
The reactions of  $[Me_3SiCH_2(Cl_2Sn)]_2(CH_2)_3$  with sodium hydroxide and of  $(PhCl_2Sn)_2CH_2$  with  $(t-Bu_2SnO)_3$  resulted in insoluble organotin oxides of unknown structures.<sup>4b,6</sup> As part of our systematic study of the influence of both R and the spacer on the structure of organotin oxides  $[(R(O)Sn)_2(CR'_2)_n]$ , we now report the syntheses and structures of the representatives with  $R = (Me_3Si)_2CH$ ,  $R' = Me, n = 1$ , and  $R = (Me_3Si)_2CH, R' = H, n = 2, 3$ .

(4) (a) Gielen, M.; Jurkschat, K. *J. Organomet. Chem.* **1984**, *273*, 303. (b) Dakternieks, D.; Jurkschat, K.; Wu, H.; Tiekkink, E. R. T. *Organometallics* **1993**, *12*, 8. (c) Dakternieks, D.; Jurkschat, K.; Schollmeyer, D.; Wu, H. *Organometallics* **1994**, *13*, 4121. (d) Tsagatakis, J. K.; Chaniotakis, N. A.; Jurkschat, K. *Helv. Chim. Acta* **1994**, *77*, 2191.

(5) Dakternieks, D.; Jurkschat, K.; Schollmeyer, D.; Wu, H. *J. Organomet. Chem.* **1995**, *492*, 145.

(6) Mehring, M.; Jurkschat, K. Unpublished results.

Chart 1



## Experimental Section

All solvents were dried and purified by standard procedures.

Bruker DPX-300 and DRX-400 spectrometers were used to obtain  $^1\text{H}$ ,  $^{13}\text{C}$ ,  $^{29}\text{Si}$ , and  $^{119}\text{Sn}$  NMR spectra.  $^1\text{H}$ ,  $^{13}\text{C}$ ,  $^{29}\text{Si}$ , and  $^{119}\text{Sn}$  chemical shifts  $\delta$  are given in ppm and are referenced against  $\text{Me}_4\text{Si}$  and  $\text{Me}_4\text{Sn}$ , respectively.  $^{119}\text{Sn}$  MAS spectra were obtained from a Bruker MSL 400 spectrometer using cross-polarization and high-power proton decoupling.  $\text{Cy}_4\text{Sn}$  was used as a secondary reference ( $\delta$  = 97.35 ppm).

The electrospray mass spectra were recorded with a Platform II single-quadrupole mass spectrometer (Micromass, Altrincham, UK) using an acetonitrile mobile phase. Acetonitrile solutions of the compounds were injected directly into the spectrometer via a Rheodyne injector equipped with a 50- $\mu\text{L}$  loop. A Harvard 22 syringe pump delivered the solutions to the vaporization nozzle of the electrospray ion source at a flow rate of 10  $\mu\text{L min}^{-1}$ . Nitrogen was used both as a drying gas and for nebulization with flow rates of approximately 200 and 20  $\text{mL min}^{-1}$ , respectively. Pressure in the mass analyzer region was usually about  $4 \times 10^{-5}$  mbar. Typically, 10 signal-averaged spectra were collected.

Molecular weight determinations were performed on a Knauer osmometer. TGA measurements were made on a Mettler instrument equipped with a PID module 200.

The density of the single crystals was determined using a Micromeritics Accu Pyc 1330.

Compounds  $(\text{Me}_3\text{Si})_2\text{CHLi}$ ,<sup>7</sup>  $(\text{Me}_2\text{ClSi})_2\text{CMe}_2$ ,<sup>8</sup> and  $(\text{Ph}_2\text{FSn})_2(\text{CH}_2)_n$  ( $n = 2, 3$ )<sup>9</sup> were prepared according to the literature.

**Synthesis of 2,2-Bis[bis(trimethylsilyl)methyldimethylstannyl]propane (1).** To a magnetically stirred solution of  $(\text{Me}_3\text{Si})_2\text{CHLi}$  (8.64 g, 52.0 mmol) in 500 mL of pentane was added in small portions at room temperature  $(\text{Me}_2\text{ClSi})_2\text{CMe}_2$  (10.00 g, 24.4 mmol). The reaction mixture was stirred overnight, and resulting LiCl was filtered off. Removing the solvent by rotary evaporation resulted in 15.38 g (96% yield) of crude product, which was recrystallized from  $\text{CH}_2\text{Cl}_2$  to give 13.10 g (yield 82%, mp 103–104 °C) of colorless crystals.  $^1\text{H}$  NMR (400.13 MHz,  $\text{CDCl}_3$ ):  $\delta$  –0.49 (s,  $^2J^{(117/119)\text{Sn}-1\text{H}}$  = 75/78 Hz, 1H, CH); 0.06 (s, 1H,  $\text{SiMe}_3$ ); 0.17 (s,  $^2J^{(117/119)\text{Sn}-1\text{H}}$  = 46 Hz, 6H,  $\text{SnMe}_2$ ); 1.43 (s,  $^3J^{(117/119)\text{Sn}-1\text{H}}$  = 76/80 Hz, 6H,  $\text{C}(\text{CH}_3)_2$ ).  $^{13}\text{C}\{\text{H}\}$  NMR (100.62 MHz,  $\text{CDCl}_3$ ):  $\delta$  –4.9 (s,  $^1J^{(117/119)\text{Sn}-13\text{C}}$  = 274/286 Hz, 4C,  $\text{SnMe}$ ); 3.76 (s,  $^1J^{(117/119)\text{Sn}-13\text{C}}$  = 124/129 Hz,  $^1J^{(29)\text{Si}-13\text{C}}$  = 39 Hz, 2C, CH); 3.7 (s,  $^1J^{(29)\text{Si}-13\text{C}}$  = 51 Hz,  $^3J^{(117/119)\text{Sn}-13\text{C}}$  = 14 Hz, 12C,  $\text{SiMe}_3$ ); 14.7 (s,  $^1J^{(117/119)\text{Sn}-13\text{C}}$  = 309/327 Hz, 1C, C); 27.7 (s,

$^2J^{(117/119)\text{Sn}-13\text{C}}$  = 19 Hz, 2C,  $\text{CH}_3$ ).  $^{29}\text{Si}\{\text{H}\}$  NMR (79.49 MHz,  $\text{CDCl}_3$ ):  $\delta$  1.37 (s,  $^2J^{(117/119)\text{Sn}-29\text{Si}}$  = 27/29 Hz,  $^1J^{(13)\text{C}-29\text{Si}}$  = 51 Hz).  $^{119}\text{Sn}\{\text{H}\}$  NMR (111.92 MHz,  $\text{CHCl}_3/\text{D}_2\text{O}_{\text{cap}}$ ):  $\delta$  32.6 (s,  $^2J^{(117)\text{Sn}-119\text{Sn}}$  = 127 Hz). Anal. Calcd for  $\text{C}_{21}\text{H}_{56}\text{Si}_2$ : C, 38.30; H, 8.57. Found: C, 38.2; H, 8.8.

### Synthesis of 2,2-Bis[bis(trimethylsilyl)methyldichlorostannyl]propane (3).

A mixture of **1** (10.71 g, 16.3 mmol) and  $\text{Me}_2\text{SnCl}_2$  (7.90 g, 36.0 mmol) was heated (110–120 °C) for 30 h to give a clear melt. The resulting  $\text{Me}_3\text{SnCl}$  was removed by sublimation (3 h,  $10^{-3}$  mmHg, 80–90 °C) to give 11.37 g (100% yield) of 2,2-bis[bis(trimethylsilyl)methyldichlorostannyl]propane (**2**) as a beige solid, which was used for the synthesis of **3** without further purification. Compound **2** consists of two diastereomers which were detected by NMR spectroscopy. However, no effort was made to assign the NMR signals to the diastereomers.  $^1\text{H}$  NMR (400.13 MHz,  $\text{CDCl}_3$ ):  $\delta$  0.14, 0.142, 0.185, 0.195 (4s, 36H,  $\text{SiMe}_3$ ); 0.256, 0.281 (2s,  $^2J^{(117/119)\text{Sn}-1\text{H}}$  = 85/90 Hz, 2H, CH); 0.743, 0.753 (2s,  $^2J^{(117/119)\text{Sn}-1\text{H}}$  = 48/50 Hz, 6H,  $\text{SnMe}$ ); 1.710, 1.725, 1.740 (3s,  $^3J^{(117/119)\text{Sn}-1\text{H}}$  = 100/115 Hz, 6H,  $\text{C}(\text{CH}_3)_2$ ).  $^{13}\text{C}\{\text{H}\}$  NMR (100.62 MHz,  $\text{CDCl}_3$ ):  $\delta$  3.33, 3.35, 3.53, 3.62 (s, 12C,  $\text{SiMe}_3$ ); 8.12 (s,  $^1J^{(117/119)\text{Sn}-13\text{C}}$  = 131/137 Hz,  $^1J^{(29)\text{Si}-13\text{C}}$  = 37 Hz, 1C, CH(a)); 8.26 (s,  $^1J^{(117/119)\text{Sn}-13\text{C}}$  = 130/136 Hz,  $^1J^{(29)\text{Si}-13\text{C}}$  = 37 Hz, 1C, CH(b)); 2.83 (s,  $^1J^{(117/119)\text{Sn}-13\text{C}}$  = 309/322 Hz, 1C,  $\text{SnMe}(a)$ ); 2.94 (s,  $^1J^{(117/119)\text{Sn}-13\text{C}}$  = 312/325 Hz, 1C,  $\text{SnMe}(b)$ ); 25.41, 25.69, 25.71, 25.77 (4s,  $^2J^{(117/119)\text{Sn}-13\text{C}}$  = 15 Hz,  $^2J^{(117/119)\text{Sn}-13\text{C}}$  = 16 Hz,  $^2J^{(117/119)\text{Sn}-13\text{C}}$  = 16 Hz,  $^2J^{(117/119)\text{Sn}-13\text{C}}$  = 19 Hz, 2C, CH); 34.98 (s,  $^1J^{(117/119)\text{Sn}-13\text{C}}$  = 333/349 Hz, C(a)); 35.04 (s,  $^1J^{(117/119)\text{Sn}-13\text{C}}$  = 336/352 Hz, C(b)).  $^{29}\text{Si}\{\text{H}\}$  NMR (79.49 MHz,  $\text{CDCl}_3$ ):  $\delta$  0.80 (s,  $^2J^{(117/119)\text{Sn}-29\text{Si}}$  = 21/22 Hz, 1Si); 0.88 (s,  $^2J^{(117/119)\text{Sn}-29\text{Si}}$  = 21/22 Hz, 1Si); 2.00 (s,  $^2J^{(117/119)\text{Sn}-29\text{Si}}$  = 40/42 Hz, 1Si); 2.07 (s,  $^2J^{(117/119)\text{Sn}-29\text{Si}}$  = 40/42 Hz, 1Si).  $^{119}\text{Sn}\{\text{H}\}$  NMR (149.21 MHz,  $\text{CDCl}_3$ ):  $\delta$  151.2 (s, 1Sn); 151.7 (s, 1Sn).

A mixture of **2** (11.37 g 16.3 mmol) and  $\text{SnCl}_4$  (8.50 g 32.6 mmol) was heated (60–70 °C) for 12 h. The resulting  $\text{Me}_2\text{SnCl}_2$  was removed by sublimation (3–4 h,  $10^{-3}$  mmHg, 80–90 °C), and the residual solid was recrystallized from hexane to give 8.9 g (74% yield) of crystalline **3**, mp 113–114 °C.  $^1\text{H}$  NMR (400.13 MHz,  $\text{CDCl}_3$ ):  $\delta$  0.25 (s, 18H,  $\text{SiMe}_3$ ); 0.98 (s,  $^2J^{(117/119)\text{Sn}-1\text{H}}$  = 90/94 Hz, 1H, CH); 1.97 (s,  $^3J^{(117/119)\text{Sn}-1\text{H}}$  = 128/134 Hz, 3H,  $\text{C}(\text{CH}_3)_2$ ).  $^{13}\text{C}\{\text{H}\}$  NMR (100.62 MHz,  $\text{CDCl}_3$ ):  $\delta$  3.1 (s,  $^1J^{(29)\text{Si}-13\text{C}}$  = 52 Hz,  $^3J^{(117/119)\text{Sn}-13\text{C}}$  = 26 Hz, 12C,  $\text{SiMe}_3$ ); 21.4 (s,  $^1J^{(117/119)\text{Sn}-13\text{C}}$  = 154/160 Hz,  $^1J^{(29)\text{Si}-13\text{C}}$  = 34 Hz, 2C, CH); 25.0 (s,  $^2J^{(117/119)\text{Sn}-13\text{C}}$  = 21 Hz, 2C, CH<sub>3</sub>); 60.2 (s,  $^1J^{(117/119)\text{Sn}-13\text{C}}$  = 412/431 Hz, 1C, C).  $^{29}\text{Si}\{\text{H}\}$  NMR (79.49 MHz,  $\text{CDCl}_3$ ):  $\delta$  1.89 (s,  $^2J^{(117/119)\text{Sn}-29\text{Si}}$  = 48/50 Hz,  $^1J^{(13)\text{C}-29\text{Si}}$  = 52 Hz).  $^{119}\text{Sn}\{\text{H}\}$  NMR (149.21 MHz,  $\text{CDCl}_3$ ):  $\delta$  78.7 (s,  $^2J^{(117)\text{Sn}-119\text{Sn}}$  = 599 Hz). Anal. Calcd for  $\text{C}_{17}\text{H}_{44}\text{Cl}_4\text{Si}_4\text{Sn}_2$ : C, 27.59; H, 5.99. Found: C, 27.5; H, 6.1.

**Synthesis of 1,2-Bis[bis(trimethylsilyl)methyldichlorostannyl]ethane (6) and 1,3-Bis[bis(trimethylsilyl)methyldichlorostannyl]propane (7).** To a magnetically stirred suspension of  $(\text{Me}_3\text{Si})_2\text{CHLi}$  (5.00 g, 30.1 mmol) in 500 mL of pentane was added in small portions at room temperature  $(\text{Ph}_2\text{FSn})_2(\text{CH}_2)_2$  (9.00 g, 14.7 mmol) or  $(\text{Ph}_2\text{FSn})_2(\text{CH}_2)_3$  (9.10 g, 14.6 mmol). The reaction mixture was stirred overnight, and the LiF was filtered. The solvent was removed in vacuo to give 11.60 g of 1,2-bis[bis(trimethylsilyl)methyldiphenylstannyl]ethane (**4**) or 10.80 g of 1,3-bis[bis(trimethylsilyl)methyldiphenylstannyl]propane (**5**), respectively, which were used for the synthesis of **6** and **7**, respectively, without further purification.  $^{13}\text{C}\{\text{H}\}$  NMR (100.62 MHz,  $\text{CDCl}_3$ ): **4**,  $\delta$  0.71 (s, 1C, CH); 3.34 (s,  $^1J^{(29)\text{Si}-13\text{C}}$  = 52 Hz,  $^3J^{(117/119)\text{Sn}-13\text{C}}$  = 16 Hz, 6C,  $\text{SiMe}_3$ ); 11.16 (s,  $^1J^{(117/119)\text{Sn}-13\text{C}}$  = 329/344 Hz,  $^2J^{(117/119)\text{Sn}-13\text{C}}$  = 43 Hz, 1C,  $\text{SnCH}_2$ ); 128.20 (s, 4C,  $\text{C}_m$ ); 128.40 (s, 2C,  $\text{C}_p$ ); 137.10 (s,  $^2J^{(117/119)\text{Sn}-13\text{C}}$  = 34 Hz, 4C,  $\text{C}_0$ ); 141.16 (s,  $^1J^{(117/119)\text{Sn}-13\text{C}}$  = 421/440 Hz, 2C,  $\text{C}_i$ ).  $^{29}\text{Si}\{\text{H}\}$  NMR (79.49 MHz,  $\text{CDCl}_3$ ): **4**,  $\delta$  1.5 (s,  $^2J^{(117/119)\text{Sn}-29\text{Si}}$  = 29/

(7) Davidson, P. J.; Harris, D. H.; Lappert, M. F. *J. Chem. Soc., Dalton Trans.* **1976**, 2268.

(8) Karol, T. J.; Hutchinson, J. P.; Hyde, J. R.; Kuivila, H. G.; Zubietta, J. A. *Organometallics* **1983**, 2, 106.

(9) Dakternieks, D.; Jurkschat, K.; Zhu, H.; Tiekkink, E. R. T. *Organometallics* **1995**, 14, 2512.

31 Hz,  $^1J(^{13}C-^{29}Si) = 52$  Hz); **5**,  $\delta$  1.3 (s,  $^2J(^{117/119}Sn-^{29}Si) = 30$  Hz,  $^1J(^{13}C-^{29}Si) = 51$  Hz).  $^{119}Sn\{^1H\}$  NMR (111.92 MHz,  $CHCl_3/D_2O_{cap.}$ ): **4**,  $\delta$  -62.0 (s,  $^3J(^{117}Sn-^{119}Sn) = 1332$  Hz); **5**,  $\delta$  -69.0 (s,  $^4J(^{117}Sn-^{119}Sn) = 99$  Hz,  $^1J(^{13}C-^{119}Sn) = 449$  Hz).

To a magnetically stirred ice-cooled solution of **4** (10.00 g, 11.2 mmol) or **5** (10.16 g, 11.2 mmol) in 100 mL of acetone was added dropwise a solution of  $HgCl_2$  (12.17 g, 44.9 mmol) in 40 mL of acetone during 1 h. The resulting white suspension was stirred overnight at room temperature. The precipitate of  $PhHgCl$  was filtered, and the solvent was removed in vacuo. The resulting residue was extracted with hexane in a Soxhlet apparatus over a period of 16 h. The hexane was removed in vacuo, and the remaining crude product was recrystallized from diethyl ether to give 5.94 g (73%) of **6** of mp 115–117 °C or 7.17 g (86.5%) of **7** of mp 85–91 °C, respectively.  $^1H$  NMR (400.13 MHz,  $CDCl_3$ ): **6**,  $\delta$  0.23 (s, 18H,  $SiMe_3$ ); 0.7 (s,  $^2J(^{117/119}Sn-^1H) = 101/105$  Hz, 1H, CH); 2.15 (s, 2H,  $SnCH_2$ ); **7**,  $\delta$  0.22 (s, 18H,  $SiMe_3$ ); 0.56 (s,  $^2J(^{117/119}Sn-^1H) = 103/108$  Hz, 1H, CH); 1.81 (t,  $^3J(^1H-^1H) = 8$  Hz,  $^2J(^{117/119}Sn-^1H) = 48$  Hz, 2H,  $SnCH_2$ ); 2.35 (quint,  $^3J(^1H-^1H) = 8$  Hz,  $^3J(^{117/119}Sn-^1H) = 90$  Hz, 1H,  $CH_2$ ).  $^{13}C\{^1H\}$  NMR (100.62 MHz,  $CDCl_3$ ): **6**,  $\delta$  2.71 (s,  $^1J(^{29}Si-^{13}C) = 53$  Hz,  $^3J(^{117/119}Sn-^{13}C) = 27$  Hz, 6C,  $SiMe_3$ ); 19.05 (s,  $^1J(^{117/119}Sn-^{13}C) = 154/161$  Hz,  $^1J(^{29}Si-^{13}C) = 36$  Hz, 1C, CH); 24.65 (s,  $^1J(^{117/119}Sn-^{13}C) = 424/444$  Hz,  $^2J(^{117/119}Sn-^{13}C) = 58$  Hz, 1C,  $SnCH_2$ ); **7**,  $\delta$  2.64 (s,  $^1J(^{29}Si-^{13}C) = 52$  Hz,  $^3J(^{117/119}Sn-^{13}C) = 26$  Hz, 12C,  $SiMe_3$ ); 18.1 (s,  $^1J(^{117/119}Sn-^{13}C) = 160/168$  Hz,  $^1J(^{29}Si-^{13}C) = 36$  Hz, 2C, CH); 20.7 (s,  $^2J(^{117/119}Sn-^{13}C) = 37$  Hz, 1C,  $CH_2$ ); 31.2 (s,  $^1J(^{117/119}Sn-^{13}C) = 424/444$  Hz,  $^3J(^{117/119}Sn-^{13}C) = 95/100$  Hz, 2C,  $SnCH_2$ ).  $^{29}Si\{^1H\}$  NMR (79.49 MHz,  $CDCl_3$ ): **6**,  $\delta$  1.9 (s,  $^2J(^{117/119}Sn-^{29}Si) = 43/45$  Hz,  $^1J(^{13}C-^{29}Si) = 52$  Hz); **7**,  $\delta$  1.8 (s,  $^2J(^{117/119}Sn-^{29}Si) = 40/42$  Hz,  $^1J(^{13}C-^{29}Si) = 52$  Hz).  $^{119}Sn\{^1H\}$  NMR (149.21 MHz,  $CDCl_3$ ): **6**,  $\delta$  112.3 (s,  $^3J(^{117}Sn-^{119}Sn) = 2010$  Hz); **7**,  $\delta$  118.6. Anal. Calcd for  $C_{16}H_{42}Cl_4Si_4Sn_2$  (**6**): C, 26.47; H, 5.83. Found: C, 26.4; H, 6.0. Anal. Calcd for  $C_{17}H_{44}Cl_4Si_2Sn_2$  (**7**): C, 29.85; H, 6.48. Found: C, 29.20; H, 6.30.

**Synthesis of 1,3,5,7-Tetrakis[bis(trimethylsilyl)methyl]-9,9,10,10-tetramethyl-2,4,6,8-tetraoxa-1,3,5,7-tetrastan-naadamantane (8), 1,3,6,8-Tetrakis[bis(trimethylsilyl)-methyl]-2,7,11,12-tetraoxa-1,3,6,8-tetrastanannatricyclo-[4.4.1.1<sup>3,8</sup>]dodecane (9), and 1,3,7,9-Tetrakis[bis(trimethylsilyl)-methyl]-2,8,13,14-tetraoxa-tricyclo[7.3.1.1<sup>3,7</sup>]-1,3,7,9-tetrastanate-tradecane (10). Method A.** To a magnetically stirred solution of **3** (1.00 g, 1.35 mmol), **6** (1.00 g, 1.35 mmol), or **7** (1.00 g, 1.35 mmol) in 5 mL of toluene was added at 80 °C a solution of  $NaOH$  (0.75 g, 18.75 mmol) in 5 mL of water, and the reaction mixture was stirred overnight. The organic layer was separated, and the toluene was removed in vacuo. The crude product was recrystallized from toluene (**8** and **10**) to give 570 mg (67%) **8** of mp 227–229 °C and 750 mg (79%) **10** of mp 166–172 °C, respectively. Compound **9** could be isolated only as its hydrolysis product (**9a**) when recrystallized from  $CH_2Cl_2$  (750 mg (88%), mp 165 °C).

**Method B.** **3**, **6**, or **7** (0.10 mmol) and  $(^tBu_2SnO)_3$  (50 mg, 0.20 mmol) were dissolved in  $CDCl_3$ , and, when examined, by  $^{119}Sn$  NMR spectroscopy, gave the same resonances as were observed for the isolated solid samples prepared from Method A.

$^1H$  NMR (400.13 MHz,  $CDCl_3$ ): **8**,  $\delta$  0.01 (s,  $^2J(^{117/119}Sn-^1H) = 90/94$  Hz, 1H, CH); 0.16 (s, 18H,  $SiMe_3$ ); 1.66 (s,  $^3J(^{117/119}Sn-^1H) = 106/111$  Hz, 3H,  $C(CH_3)_2$ ); **9**,  $\delta$  -0.1 (s,  $^2J(^{117/119}Sn-^1H) = 102/107$  Hz, 1H, CH); 0.14 (s, 18H,  $SiMe_3$ ); 1.49 (s, 2H,  $SnCH_2$ ); **10**,  $\delta$  -0.23 (s,  $^2J(^{117/119}Sn-^1H) = 96/100$  Hz, 2H, CH); 0.108 (s, 18H,  $SiMe_3(a)$ ); 0.116 (s, 18H,  $SiMe_3(b)$ ); 1.08 (m,  $^2J(^{117/119}Sn-^1H) = 170$  Hz, 2H,  $SnCHH$ ); 1.35 (m,  $^2J(^{117/119}Sn-^1H) = 80$  Hz, 2H,  $SnCHH$ ); 2.30 (m,  $^3J(^{117/119}Sn-^1H) = 200$  Hz, 1H,  $CHH$ ); 2.86 (m,  $^3J(^{117/119}Sn-^1H) = 90$  Hz, 1H,  $CHH$ ).  $^{13}C\{^1H\}$  NMR (100.62 MHz,  $CDCl_3$ ): **8**,  $\delta$  3.19 (s,

$^1J(^{29}Si-^{13}C) = 52$  Hz,  $^3J(^{117/119}Sn-^{13}C) = 19$  Hz, 12C,  $SiMe_3$ ); 9.17 (s,  $^1J(^{117/119}Sn-^{13}C) = 198/208$  Hz,  $^1J(^{29}Si-^{13}C) = 38$  Hz, 2C, CH); 24.83 (s,  $^2J(^{117/119}Sn-^{13}C) = 16$  Hz, 2C,  $CH_3$ ); 47.1 (s,  $^1J(^{117/119}Sn-^{13}C) = 416/433$  Hz, 1C, C); **9**,  $\delta$  7.05 (s,  $^1J(^{29}Si-^{13}C) = 49$  Hz,  $^3J(^{117/119}Sn-^{13}C) = 20$  Hz, 6C,  $SiMe_3$ ); 15.30 (s,  $^1J(^{117/119}Sn-^{13}C) = 221/232$  Hz,  $^1J(^{29}Si-^{13}C) = 37$  Hz, 1C, CH); 21.94 (s,  $^1J(^{117/119}Sn-^{13}C) = 473/496$  Hz,  $^2J(^{117/119}Sn-^{13}C) = 30$  Hz, 1C,  $SnCH_2$ ); **10**,  $\delta$  3.21 (s,  $^1J(^{29}Si-^{13}C) = 51$  Hz,  $^3J(^{117/119}Sn-^{13}C) = 21$  Hz, 6C,  $SiMe_3(a)$ ); 3.24 (s,  $^1J(^{29}Si-^{13}C) = 51$  Hz,  $^3J(^{117/119}Sn-^{13}C) = 18$  Hz, 6C,  $SiMe_3(b)$ ); 12.34 (s,  $^1J(^{117/119}Sn-^{13}C) = 237/249$  Hz,  $^1J(^{29}Si-^{13}C) = 39$  Hz, 2C,  $CH(a,b)$ ); 20.54 (s,  $^2J(^{117/119}Sn-^{13}C) = 42$  Hz, 1C,  $CH_2(a,b)$ ); 26.61 (s,  $^1J(^{117/119}Sn-^{13}C) = 472/493$  Hz,  $^3J(^{117/119}Sn-^{13}C) = 19$  Hz, 2C,  $SnCH_2(a,b)$ ).  $^{29}Si\{^1H\}$  NMR (79.49 MHz,  $CDCl_3$ ): **8**,  $\delta$  1.23 (s,  $^2J(^{117/119}Sn-^{29}Si) = 42/44$  Hz,  $^1J(^{13}C-^{29}Si) = 51$  Hz); **9**,  $\delta$  0.67 (s,  $^2J(^{117/119}Sn-^{29}Si) = 37/39$  Hz,  $^1J(^{13}C-^{29}Si) = 51$  Hz); **10**,  $\delta$  -0.08 (s,  $^2J(^{117/119}Sn-^{29}Si) = 30/31$  Hz,  $^1J(^{13}C-^{29}Si) = 51$  Hz, 1Si,  $SiMe_3(a)$ ); 0.68 (s,  $^2J(^{117/119}Sn-^{29}Si) = 47/49$  Hz,  $^1J(^{13}C-^{29}Si) = 51$  Hz, 1Si,  $SiMe_3(b)$ ).  $^{119}Sn\{^1H\}$  NMR (149.21 MHz,  $CDCl_3$ ): **8**,  $\delta$  23.8 (s,  $^2J(^{117}Sn-O-^{119}Sn) = 390$  Hz,  $^2J(^{117}Sn-^{119}Sn) = 740$  Hz); **9**,  $\delta$  24.7 (s,  $^2J(^{117}Sn-O-^{119}Sn) = 520$  Hz,  $^3J(^{117}Sn-^{119}Sn) = 205$  Hz); **10**,  $\delta$  24.9,  $W_{1/2} = 1.2$  Hz (s,  $^2J(^{117}Sn-^{119}Sn) = 381$  Hz,  $^2J(^{117}Sn-^{119}Sn) = 495$  Hz).  $^{119}Sn$  MAS NMR (149.21 MHz): **8**,  $\delta$  24.4; **9a**,  $\delta$  -163.4; -168.5; **10**,  $\delta$  34.3 (s,  $^2J(^{117}Sn-^{119}Sn) = 436$  Hz, 1Sn); 24.0 (s,  $^2J(^{117}Sn-^{119}Sn) = 436$  Hz, 1Sn). Anal. Calcd for  $C_{34}H_{88}O_4Si_8Sn_4$  (**8**): C, 32.39; H, 7.04. Found: C, 32.4; H, 7.2. Anal. Calcd for  $C_{48}H_{136}O_{11}Si_{12}Sn_6$  (**9a**): C, 29.73; H, 7.07. Found: C, 30.02; H, 7.31. Anal. Calcd for  $C_{34}H_{88}O_4Si_8Sn_4$  (**10**): C, 32.39; H, 7.04. Found: C, 32.51; H, 7.22. Molecular mass (found in  $CH_2Cl_2$ ): **8**, 1185; **9a**, 1272 (fits for **9** in solution); **10**, 1208 g/mol. DTA: **9a**, 95–155 °C, loss of 5  $H_2O$ .

**Synthesis of 2,6-Dichloro-2,6-bis[bis(trimethylsilyl)-methyl]-1-oxa-2,6-distannacyclohexane (11). Method A.** Compounds **10** (50 mg, 0.040 mmol) and **7** (59 mg, 0.080 mmol) were dissolved in  $CDCl_3$ . After 24 h, the precipitate (95 mg, 87%) of colorless crystals of **11** was collected, mp 113–122 °C.  $^{13}C\{^1H\}$  NMR (100.62 MHz,  $CDCl_3$ ):  $\delta$  2.77 (s,  $^1J(^{29}Si-^{13}C) = 52$  Hz,  $^3J(^{117/119}Sn-^{13}C) = 25$  Hz, 12C,  $SiMe_3$ ); 16.94 (s, 2C, CH); 21.48 (s,  $^2J(^{117/119}Sn-^{13}C) = 46$  Hz, 1C,  $CH_2$ ); 29.18 (s, 2C,  $SnCH_2$ ).  $^{119}Sn\{^1H\}$  NMR (149.21 MHz,  $CDCl_3$ ):  $\delta$  86.4 (s, 14%); 78.97 (s, 86%). Anal. Calcd for  $C_{17}H_{44}Cl_2OSi_4Sn_2$ : C, 29.80; H, 6.47. Found: C, 29.83; H, 6.71. Molecular weight found in  $CH_2Cl_2$ : 687.

**Method B (in situ generation of 11).** **12** (89 mg, 0.12 mmol) and  $(t-Bu_2SnO)_3$  (30 mg, 0.04 mmol) were dissolved in  $CDCl_3$ , and the resulting clear solution was examined by  $^{119}Sn$  NMR spectroscopy.  $^{119}Sn\{^1H\}$  NMR (149.21 MHz,  $CDCl_3$ ):  $\delta$  86.1 (s, 15%); 71.6 (s, 85%); 54.6 (s,  $t-Bu_2SnCl_2$ ).

**Synthesis of 2,6-Difluoro-2,6-bis[bis(trimethylsilyl)-methyl]-1-oxa-2,6-distannacyclohexane Dimer (12).** To a magnetically stirred solution of **7** (0.61 g, 0.82 mmol) in 10 mL of diethyl ether was added excess potassium fluoride (3.00 g, 61.0 mmol), dissolved in 10 mL of water. The reaction mixture was stirred for 5 d at room temperature. The ether was removed in vacuo, and the resulting precipitate was filtered and washed three times with water in order to remove traces of KF and KCl. Recrystallization from chloroform afforded colorless crystals of **12** (0.52 g, 89%) of mp 294–298 °C. Anal. Calcd for  $C_{34}H_{88}F_4O_2Si_8Sn_4$ : C, 31.30; H, 6.80. Found: C, 31.21; H, 7.52. There are two sets of NMR signals.

**Set 1.**  $^{19}F$  NMR (282.4 MHz,  $CDCl_3$ ):  $\delta$   $^{19}F_a$  -134.3 ppm, d,  $^2J(^{19}F_a-^{19}F_b) = 59$  Hz,  $^1J(^{117/119}Sn-^{19}F_a) = 2643/2762$  Hz;  $\delta$   $^{19}F_b$  -85.5 ppm, d,  $^2J(^{19}F_a-^{19}F_b) = 59$  Hz,  $^1J(^{117/119}Sn-^{19}F_b) = 1270$  Hz.  $^{119}Sn\{^1H\}$  NMR (149.21 MHz,  $CDCl_3$ ):  $\delta$   $^{119}Sn(I) = -153.8$  ppm, dd,  $^1J(^{119}Sn(I)-^{19}F_a) = 2765$  Hz,  $^1J(^{119}Sn(I)-^{19}F_b) = 1255$  Hz,  $^2J(^{119}Sn(I)-^{117/119}Sn(II)) = 215$  Hz;  $\delta$   $^{119}Sn(II) = -115.1$  ppm, ddd,  $^1J(^{119}Sn(II)-^{19}F_b) = 1483$  Hz,  $^3J(^{119}Sn(II)-^{19}F_a) = 33$  Hz,  $^3J(^{119}Sn(II)-^{19}F_b) = 19$  Hz.

**Set 2.**  $^{19}F$  NMR (282.4 MHz,  $CDCl_3$ ):  $\delta$   $^{19}F_a$  -133.8 ppm, d,  $^2J(^{19}F_a-^{19}F_b) = 62$  Hz,  $^1J(^{117/119}Sn-^{19}F_a) = 2700/2825$  Hz;  $\delta$

**Table 1.** Crystallographic Data for **2**, **6**, **8**, **9a**, **10**, and **12**

	<b>3</b>	<b>6</b>	<b>8</b>	<b>9a</b>	<b>10</b>	<b>12</b>
formula	C <sub>17</sub> H <sub>44</sub> Cl <sub>4</sub> Si <sub>4</sub> Sn <sub>2</sub>	C <sub>16</sub> H <sub>42</sub> Cl <sub>4</sub> Si <sub>4</sub> Sn <sub>2</sub>	C <sub>34</sub> H <sub>88</sub> O <sub>4</sub> Si <sub>8</sub> Sn <sub>4</sub>	C <sub>48</sub> H <sub>132</sub> O <sub>9</sub> Si <sub>12</sub> Sn <sub>6</sub> ·2H <sub>2</sub> O	C <sub>34</sub> H <sub>88</sub> O <sub>4</sub> Si <sub>8</sub> Sn <sub>4</sub>	C <sub>34</sub> H <sub>88</sub> O <sub>4</sub> Si <sub>8</sub> Sn <sub>4</sub> ·3CHCl <sub>3</sub>
fw	740.06	726.04	1260.52	1938.79	1260.52	1662.63
cryst syst	monoclinic	monoclinic	tetragonal	triclinic	monoclinic	monoclinic
cryst size, mm	0.25 × 0.20 × 0.20	0.23 × 0.20 × 0.20	0.28 × 0.28 × 0.25	0.12 × 0.10 × 0.10	0.20 × 0.15 × 0.12	0.40 × 0.20 × 0.20
space group	P <sub>2</sub> 1/c	P <sub>2</sub> 1/c	P4 <sub>2</sub> 2,2	P-1	P2 <sub>1</sub> /n	C2/c
<i>a</i> , Å	19.288(1)	12.043(1)	16.044(2)	9.233(1)	12.335(2)	32.423(1)
<i>b</i> , Å	12.703(1)	17.284(1)	16.044(2)	17.048(1)	16.616(2)	9.723(1)
<i>c</i> , Å	13.592(1)	15.578(1)	22.914(3)	29.144(1)	14.535(2)	26.891(1)
$\alpha$ , deg	90	90	90	87.050(1)	90	90
$\beta$ , deg	101.517(1)	107.817(1)	90	87.601(1)	99.58(1)	123.038(1)
$\gamma$ , deg	90	90	90	77.645(1)	90	90
<i>V</i> , Å <sup>3</sup>	3263.2(4)	3087.1(4)	5897.3(13)	4473.0(6)	2935.7(9)	7097.1(8)
<i>Z</i>	4	4	4	2	2	4
$\rho_{\text{calcd}}$ , Mg/m <sup>3</sup>	1.506	1.562	1.419	1.440	1.426	1.556
$\rho_{\text{meas}}$ , Mg/m <sup>3</sup>	1.510(3)	1.557(3)	1.419(5)	1.456(3)	1.431(4)	nm <sup>a</sup>
$\mu$ , mm <sup>-1</sup>	2.010	2.123	1.865	1.850	1.873	1.556
<i>F</i> (000)	1480	1448	2544	1960	1272	3320
$\theta$ range, deg	4.43–25.64	4.61–25.66	3.10–27.47	4.80–24.72	3.10–24.97	2.23–26.36
index ranges	-20 ≤ <i>h</i> ≤ 20 -15 ≤ <i>k</i> ≤ 15 -16 ≤ <i>l</i> ≤ 16	-14 ≤ <i>h</i> ≤ 14 -21 ≤ <i>k</i> ≤ 21 -18 ≤ <i>l</i> ≤ 18	-2 ≤ <i>h</i> ≤ 20 -2 ≤ <i>k</i> ≤ 20 -2 ≤ <i>l</i> ≤ 29	-10 ≤ <i>h</i> ≤ 10 -15 ≤ <i>k</i> ≤ 20 -33 ≤ <i>l</i> ≤ 34	-1 ≤ <i>h</i> ≤ 14 -1 ≤ <i>k</i> ≤ 19 -17 ≤ <i>l</i> ≤ 17	-38 ≤ <i>h</i> ≤ 38 -10 ≤ <i>k</i> ≤ 10 -31 ≤ <i>l</i> ≤ 26
no. of reflns collectd	45 282	42 766	10 357	12 590	6364	47 422
completeness to	93.1	100.0	100.0	45.1	100.0	87.9
$\theta_{\text{max}}$						
no. of indep reflns/	5749/0.036	5799/0.042	6752/0.094	6819/0.050	5159/0.043	6373/0.035
$R_{\text{int}}$						
no. of reflns obsd with ( <i>I</i> > 2 <i>σ</i> ( <i>I</i> ))	3925	3883	2549	3728	2965	4354
absorpn correction	none	none	Psi-Scan 1.000/0.919	none	Psi-Scan 1.000/0.874	none
<i>T</i> <sub>max</sub> / <i>T</i> <sub>min</sub>						
no. of refined params	245	248	241	732	239	370
GooF ( <i>F</i> <sup>2</sup> )	0.912	0.905	0.991	1.048	1.012	0.942
<i>R</i> 1 ( <i>F</i> ) ( <i>I</i> > 2 <i>σ</i> ( <i>I</i> ))	0.0265	0.0292	0.0729	0.0585	0.0458	0.0309
wR2 ( <i>F</i> <sup>2</sup> ) (all data)	0.0574	0.0571	0.1089	0.1207	0.1065	0.0683
( $\Delta/\sigma$ ) <sub>max</sub>	0.001	0.001	<0.001	0.001	<0.001	0.001
largest diff peak/hole, e/Å <sup>3</sup>	0.311/-0.401	0.381/-0.621	0.484/-0.512	0.367/-0.339	0.967/-0.497	0.556/-0.726

<sup>a</sup> Not measured.

<sup>19</sup>F<sub>b</sub> –71.9 ppm, broad, <sup>1</sup>J(<sup>117/119</sup>Sn–<sup>19</sup>F<sub>b</sub>) = 1360 Hz. <sup>119</sup>Sn-{<sup>1</sup>H} NMR (149.21 MHz, CDCl<sub>3</sub>): δ <sup>119</sup>Sn(I) –153.7 ppm, dd, <sup>1</sup>J(<sup>119</sup>Sn(I)–<sup>19</sup>F<sub>a</sub>) = 2820 Hz, <sup>1</sup>J(<sup>119</sup>Sn(I)–<sup>19</sup>F<sub>b</sub>) = 1190 Hz <sup>2</sup>J(<sup>119</sup>Sn(I)-<sup>117/119</sup>Sn(II)) = 215 Hz; δ <sup>119</sup>Sn(II) –108.4 ppm, dd, <sup>1</sup>J(<sup>119</sup>Sn(II)–<sup>19</sup>F<sub>b</sub>) = 1537 Hz <sup>3</sup>J(<sup>119</sup>Sn(II)–<sup>19</sup>F<sub>a</sub>) = 33 Hz.

**Crystallography.** Intensity data for the colorless crystals were collected on Nonius MACH3 (**8**, **10**) and KappaCCD (**3**, **6**, **9a**, **12**) diffractometers with graphite-monochromated Mo Kα radiation (0.710 69 Å) at 291 (**3**, **6**, **8**, **9a**, **10**) and 200 K (**12**). Three standard reflections were recorded every 60 min (**8**, **10**), and anisotropic intensity losses up to 28.6% (**8**) and 14.3% (**10**) were detected during X-ray exposure. The data collections for (**3**, **6**, **9a**, **12**) covered the sphere of reciprocal space with 360 frames via  $\omega$ -rotation ( $\Delta/\omega = 1^\circ$ ) (**3**, **6**, **12**) and with 720 frames via  $\omega$ -rotation ( $\Delta/\omega = 0.5^\circ$ ) (**9a**) at two times 5*s* (**6**), 8*s* (**12**), and 10*s* (**3**, **9a**) per frame. The crystal-to-detector distance was 2.6 (**5**, **10**), 2.7 (**9a**), and 2.9 cm (**12**). Crystal decay was monitored by repeating the initial frames at the end of data collection. On analyzing the duplicate reflections, there was no indication for any decay (**3**, **6**, **9a**, **12**). The structures were solved by direct methods SHELXS86<sup>10a</sup> and successive difference Fourier syntheses. Refinement applied full-matrix least-squares methods SHELXL93.<sup>10b</sup>

The H atoms were placed in geometrically calculated positions using a riding model and refined with a common isotropic temperature factor (C<sub>prim</sub>.–H 0.96, C<sub>sec</sub>.–H 0.97, and C<sub>tert</sub>.–H 0.98 Å; *U*<sub>iso</sub> = 0.119(2) (**3**), 0.088(2) (**6**), 0.0152(9) (**8**), 0.118(6) (**9a**), 0.127(6) (**10**), 0.110(3) (**12**) Å<sup>2</sup>).

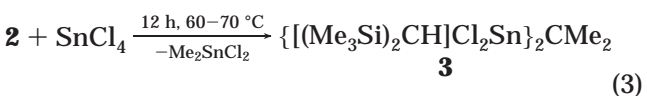
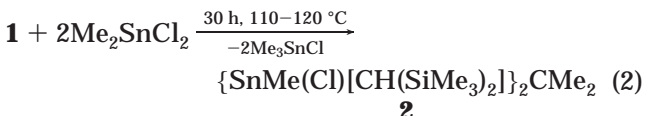
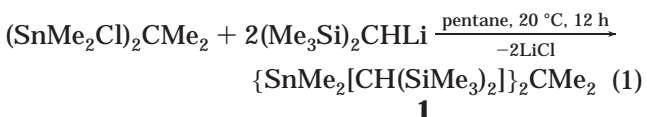
The absolute configuration for **8** was confirmed by refinement of the Flack<sup>10c</sup> parameter, 0.04(5).

(10) (a) Sheldrick, G. M. *Acta Crystallogr.* **1990** A46, 467–473. (b) Sheldrick, G. M. University of Göttingen, 1993. (c) Flack, H. D. *Acta Crystallogr.* **1983** A39, 876–881. (d) *International Tables for Crystallography*; Kluwer Academic Publishers: Dordrecht, 1992; Vol. C. (e) Sheldrick, G. M. *SHELXTL-Plus*, Release 4.1; Siemens Analytical X-ray Instruments Inc., Madison, WI, 1991.

Atomic scattering factors for neutral atoms and real and imaginary dispersion terms were taken from ref 10d. Figures were created by SHELXTL-Plus.<sup>10e</sup> Crystallographic data are given in Table 1, while selected bond distances and bond angles are listed in Tables 2 (**3**, **6**), 3 (**8**, **10**), 4 (**9a**), and 5 (**12**).

## Results and Discussion

**Synthesis of the Spacer-Bridged Ditin Compounds 1–7 and Molecular Structures of the Bis-(organodichlorostannylyl)alkanes **3** and **6**.** The reaction of (Me<sub>2</sub>ClSn)<sub>2</sub>CMe<sub>2</sub><sup>8</sup> with (Me<sub>3</sub>Si)<sub>2</sub>CHLi<sup>7</sup> afforded {Me<sub>2</sub>[(Me<sub>3</sub>Si)<sub>2</sub>CH]Sn}<sub>2</sub>CMe<sub>2</sub> (**1**, eq 1), which was converted into its tetrachloro derivative {[Me<sub>3</sub>Si]<sub>2</sub>CHCl<sub>2</sub>Sn}<sub>2</sub>CMe<sub>2</sub> (**3**) by stepwise reaction with Me<sub>2</sub>SnCl<sub>2</sub> and SnCl<sub>4</sub> (eqs 2 and 3).



The di- and trimethylene bridged ditin compounds, **6** and **7**, respectively, were prepared by reaction of (Ph<sub>2</sub>FSn)<sub>2</sub>(CH<sub>2</sub>)<sub>n</sub> (*n* = 2, 3)<sup>9</sup> with (Me<sub>3</sub>Si)<sub>2</sub>CHLi<sup>7</sup> (eq 4),

**Table 2. Selected Interatomic Bond Distances (Å) and Angles (deg) for **3** and **6****

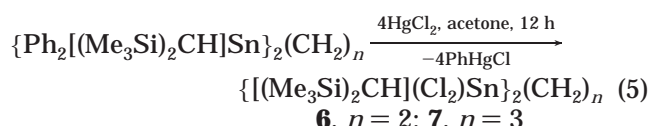
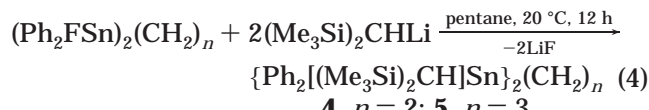
	<b>3</b>	<b>6</b>		<b>3</b>	<b>6</b>
Bond Distances					
Sn(1)–C(1)	2.125(3)	2.132(3)	Sn(2)–C(2)	2.177(3)	
Sn(1)–C(2)	2.167(3)	2.146(3)	Sn(2)–C(3)		2.151(3)
Sn(1)–Cl(1)	2.3562(9)	2.356(1)	Sn(2)–C(4)		2.123(3)
Sn(1)–Cl(2)	2.3593(9)	2.3460(9)	Sn(2)–C(5)	2.125(3)	
Sn(1)–Cl(4)	3.637(1)		Sn(2)–Cl(3)	2.359(1)	2.334(1)
Sn(2)–Cl(2)	3.467(1)		Sn(2)–Cl(4)	2.357(1)	2.355(1)
Bond Angles					
C(1)–Sn(1)–C(2)	124.0(1)	124.3(1)	C(5)–Sn(2)–Cl(3)	107.0(1)	
C(1)–Sn(1)–Cl(1)	108.30(9)	107.38(9)	C(5)–Sn(2)–Cl(4)	114.63(9)	
C(1)–Sn(1)–Cl(2)	114.57(9)	111.90(8)	Cl(3)–Sn(2)–Cl(4)	100.77(4)	101.11(4)
C(2)–Sn(1)–Cl(1)	107.07(9)	105.7(1)	C(3)–Sn(2)–C(4)		124.6(1)
C(2)–Sn(1)–Cl(2)	102.16(9)	104.5(1)	C(3)–Sn(2)–Cl(3)		103.3(1)
Cl(1)–Sn(1)–Cl(2)	97.33(3)	100.40(4)	C(3)–Sn(2)–Cl(4)		105.7(1)
C(2)–Sn(2)–C(5)	131.2(1)		C(4)–Sn(2)–Cl(3)		111.50(9)
C(2)–Sn(2)–Cl(3)	102.06(9)		C(4)–Sn(2)–Cl(4)		108.05(9)
C(2)–Sn(2)–Cl(4)	96.2(1)				

**Table 3. Selected Interatomic Bond Distances (Å) and Angles (deg) for **8** and **10<sup>a</sup>****

	<b>8</b>	<b>10</b>		<b>8</b>	<b>10</b>
Bond Distances					
Sn(1)–O(1)	1.963(5)	1.971(4)	Sn(2)–O(2a)		1.955(4)
Sn(1)–O(2)	1.973(7)	1.961(4)	Sn(2)–O(2)	1.982(7)	
Sn(1)–C(1)		2.144(7)	Sn(2)–O(3)	1.950(5)	
Sn(1)–C(1a)	2.18(1)		Sn(2)–C(1)	2.14(1)	
Sn(1)–C(10)	2.15(1)	2.133(6)	Sn(2)–C(3)		2.141(7)
Sn(2)–O(1)		1.970(4)	Sn(2)–C(20)	2.17(1)	2.143(6)
Bond Angles					
O(1)–Sn(1)–O(2)	103.0(2)	104.7(2)	O(2)–Sn(2)–C(20)	112.7(4)	
O(1)–Sn(1)–C(1a)	108.6(3)		O(3)–Sn(2)–C(1)	107.7(3)	
O(1)–Sn(1)–C(10)	109.8(4)	110.0(2)	O(3)–Sn(2)–C(20)	112.7(4)	
O(2)–Sn(1)–C(1a)	103.6(3)		C(1)–Sn(1)–C(20)	114.4(4)	
O(2)–Sn(1)–C(10)	111.6(4)	107.3(2)	O(1)–Sn(2)–C(20)		107.6(2)
O(1)–Sn(1)–C(1)		106.7(2)	O(2a)–Sn(2)–C(3)		108.1(3)
O(2)–Sn(1)–C(1)		107.9(3)	O(2a)–Sn(2)–C(20)		108.1(2)
C(1)–Sn(1)–C(10)		119.2(3)	C(3)–Sn(2)–C(20)		120.0(3)
C(1a)–Sn(1)–C(10)	118.9(4)		Sn(1)–O(1)–Sn(2)	124.0(4)	122.1(2)
O(1)–Sn(2)–O(2a)		105.6(2)	Sn(1)–O(2)–Sn(2a)		128.5(2)
O(1)–Sn(2)–C(3)		106.6(3)	Sn(1)–O(2)–Sn(1a)	121.3(5)	
O(2)–Sn(2)–O(3)	101.8(2)		Sn(2)–O(3)–Sn(2a)	121.9(5)	
O(2)–Sn(2)–C(1)	106.5(4)		Sn(2)–C(1)–Sn(1a)	106.9(4)	

<sup>a</sup>  $a = -X, -Y, -Z + 0.5$  (**8**);  $a = -X, -Y, -Z + 1$  (**10**).

followed by treatment with mercuric chloride (eq 5).



Compounds **1**–**7** are colorless crystalline solids which are very soluble in organic solvents. As expected, **2** consists of a mixture of diastereomers, as was evidenced by the observation of two almost equally intense <sup>119</sup>Sn NMR resonances at 151.2 and 151.7 ppm. No attempt was made to separate these diastereomers.

The molecular structures of **3** and **6** are shown in Figures 1 and 2, respectively. Selected bond lengths and bond angles are listed in Table 2. In **3**, both Sn(1) and Sn(2) show geometries along the path tetrahedron–trigonal bipyramidal induced by weak intramolecular Sn(1)…Cl(4) and Sn(2)…Cl(2) contacts of 3.630(3) and 3.456(3) Å. These contacts are shorter than the sum of

the van der Waals radii of tin (2.20 Å)<sup>11</sup> and chlorine (1.70–1.90 Å)<sup>11</sup> and are made possible by opening of the C(1)–Sn(1)–C(2) and C(2)–Sn(2)–C(5) angles to 123.4–133.2(4)°, respectively. A quantitative measure of the position of a real structure along the path tetrahedron–trigonal bipyramidal is the difference of the sums of the equatorial and axial angles,  $\sum \vartheta_{\text{eq}} - \sum \vartheta_{\text{ax}}$ ,<sup>12</sup> it amounts to 26.1° for Sn(1) and 32.44 for Sn(2). In the dimethylene-bridged compound **6**, both tin atoms are essentially tetracoordinate, there being no intra- or intermolecular Sn…Cl interactions. The Sn–C and Sn–Cl bond lengths in both **3** and **6** are as expected and comparable with those of related compounds.<sup>13</sup>

**Syntheses of the Molecular Organotin Oxides **8**–**10** and Molecular Structures of **8** and **10**.** Compounds **3**, **6**, and **7** are easily transformed into the corresponding diorganotin oxides **8**, **9**, and **10**, respectively (Scheme 1).

(11) Huheey, J. E.; Keiter, E. A.; Keiter, R. L. *Anorganische Chemie: Prinzipien von Struktur und Reaktivität*, 2nd ed.; de Gruyter: Berlin, New York, 1995; p 335.

(12) (a) Kolb, U.; Dräger, M.; Joussemae, B. *Organometallics* **1991**, *10*, 2737. (b) Kolb, U.; Beuter, M.; Dräger, M. *Inorg. Chem.* **1994**, *33*, 4522.

(13) Dakternieks, D.; Jurkschat, K.; Tiekkink, E. R. T. *Main Group Metal Chem.* **1994**, *17*, 471 and references cited.

**Table 4.** Selected Interatomic Bond Distances ( $\text{\AA}$ ) and Angles (deg) for **9a**

Bond Distances					
Sn(1)–O(1)	2.22(1)	Sn(3)–O(2')	1.98(1)	Sn(5)–C(5)	2.15(2)
Sn(1)–O(6)	2.193(9)	Sn(3)–O(3)	2.195(9)	Sn(5)–C(5')	2.14(1)
Sn(1)–O(6')	1.980(9)	Sn(3)–C(3)	2.15(1)	Sn(6)–O(5)	2.19(1)
Sn(1)–C(1)	2.15(2)	Sn(3)–C(3')	2.13(2)	Sn(6)–O(6)	2.26(1)
Sn(1)–C(1')	2.19(2)	Sn(4)–Sn(5)	3.251(2)	Sn(6)–O(6')	1.994(8)
Sn(2)–Sn(3)	3.261(2)	Sn(4)–O(3)	2.157(8)	Sn(6)–C(6)	2.17(1)
Sn(2)–O(1)	2.15(1)	Sn(4)–O(4)	2.244(9)	Sn(6)–C(6')	2.13(2)
Sn(2)–O(2)	2.26(1)	Sn(4)–C(4)	2.13(1)	O(1)···O(7)	2.77(2)
Sn(2)–O(2')	1.98(1)	Sn(4)–C(4')	2.14(2)	O(2')···O(7)	2.79(2)
Sn(2)–C(2)	2.15(2)	Sn(5)–O(4)	2.23(1)	O(4')···O(8)	2.84(2)
Sn(2)–C(2')	2.14(1)	Sn(5)–O(4')	1.987(9)	O(5)···O(8)	2.98(2)
Sn(3)–O(2)	2.19(1)	Sn(5)–O(5)	2.15(1)	O(6')···O(7)	2.71(2)
				O(7)···O(8)	2.78(2)
Bond Angles					
O(6')–Sn(1)–C(1)	107.3(5)	O(2)–Sn(3)–O(3)	166.0(4)	C(6)–Sn(6)–O(6)	90.1(5)
O(6')–Sn(1)–C(1')	124.6(4)	O(4')–Sn(4)–C(4)	122.7(6)	O(5)–Sn(6)–O(6)	162.3(4)
C(1)–Sn(1)–C(1')	128.1(5)	O(4')–Sn(4)–C(4')	115.8(5)	Sn(1)–O(1)–O(7)	99.4(4)
O(6')–Sn(1)–O(6)	77.0(4)	C(4)–Sn(4)–C(4')	121.1(7)	Sn(3)–O(2)–Sn(2)	94.2(3)
C(1)–Sn(1)–O(6)	94.8(5)	O(4')–Sn(4)–O(3)	88.3(4)	Sn(3)–O(2')–Sn(2)	110.7(4)
C(1')–Sn(1)–O(6)	96.4(5)	C(4)–Sn(4)–O(3)	87.4(5)	Sn(3)–O(2')–O(7)	136.8(5)
O(6')–Sn(1)–O(1)	87.4(4)	C(4)–Sn(4)–O(3)	100.8(5)	Sn(2)–O(2')–O(7)	105.1(5)
C(1)–Sn(1)–O(1)	87.8(5)	O(4')–Sn(4)–O(4)	75.8(4)	Sn(4)–O(3)–Sn(3)	118.1(4)
C(1')–Sn(1)–O(1)	94.1(4)	C(4)–Sn(4)–O(4)	92.2(5)	Sn(5)–O(4)–Sn(4)	93.3(3)
O(6)–Sn(1)–O(1)	164.2(4)	C(4')–Sn(4)–O(4)	96.0(5)	Sn(4)–O(4')–Sn(5)	110.0(4)
O(2')–Sn(2)–C(2')	114.7(5)	O(3)–Sn(4)–O(4)	160.7(4)	Sn(4)–O(4')–O(8)	143.5(5)
O(2')–Sn(2)–C(2)	117.7(5)	O(4')–Sn(5)–C(5')	122.7(5)	Sn(5)–O(4')–O(8)	106.5(5)
C(2')–Sn(2)–C(2)	126.7(6)	O(4')–Sn(5)–C(5)	109.7(5)	Sn(5)–O(5)–Sn(6)	117.5(4)
O(2')–Sn(2)–O(1)	90.2(4)	C(5')–Sn(5)–C(5)	127.6(6)	Sn(5)–O(5)–O(8)	97.8(6)
C(2')–Sn(2)–O(1)	100.6(5)	O(4')–Sn(5)–O(5)	89.1(4)	Sn(6)–O(5)–O(8)	126.7(5)
C(2)–Sn(2)–O(1)	88.5(5)	C(5')–Sn(5)–O(5)	94.3(5)	Sn(1)–O(6)–Sn(6)	93.9(4)
O(2')–Sn(2)–O(2)	75.1(4)	C(5)–Sn(5)–O(5)	87.5(6)	Sn(1)–O(6')–Sn(6)	109.9(5)
C(2')–Sn(2)–O(2)	94.6(5)	O(4')–Sn(5)–O(4)	76.0(4)	Sn(1)–O(6')–O(7)	108.4(4)
C(2)–Sn(2)–O(2)	89.6(5)	C(5')–Sn(5)–O(4)	97.1(5)	Sn(6)–O(6')–O(7)	133.9(5)
O(1)–Sn(2)–O(2)	162.3(3)	C(5)–Sn(5)–O(4)	93.6(6)	O(6')–O(7)–O(1)	64.0(4)
O(2)–Sn(3)–C(3')	124.3(5)	O(5)–Sn(5)–O(4)	164.6(3)	O(6')–O(7)–O(8)	95.5(5)
O(2')–Sn(3)–C(3)	108.6(6)	O(6')–Sn(6)–C(6')	115.4(5)	O(1)–O(7)–O(8)	159.1(6)
C(3')–Sn(3)–C(3)	127.0(7)	O(6')–Sn(6)–C(6)	120.2(5)	O(6')–O(7)–O(2')	105.6(5)
O(2')–Sn(3)–O(2)	76.8(4)	C(6')–Sn(6)–C(6)	123.8(6)	O(1)–O(7)–O(2')	63.6(4)
C(3')–Sn(3)–O(2)	96.7(5)	O(6')–Sn(6)–O(5)	91.1(4)	O(8)–O(7)–O(2')	122.6(7)
C(3)–Sn(3)–O(2)	92.8(4)	C(6')–Sn(6)–O(5)	99.7(5)	O(7)–O(8)–O(4')	88.5(5)
O(2')–Sn(3)–O(3)	89.5(4)	C(6)–Sn(6)–O(5)	87.1(6)	O(7)–O(8)–O(5)	86.1(5)
C(3')–Sn(3)–O(3)	93.4(5)	O(6')–Sn(6)–O(6)	75.2(4)	O(4')–O(8)–O(5)	59.9(4)
C(3)–Sn(3)–O(3)	88.8(4)	C(6')–Sn(6)–O(6)	96.3(5)		

**Table 5.** Selected Interatomic Bond Distances ( $\text{\AA}$ ) and Angles (deg) for **12<sup>a</sup>**

Bond Distances					
Sn(1)–F(1)	2.141(2)	Sn(1)–O(1a)	2.127(2)	Sn(2)–F(2)	1.993(2)
Sn(1)–F(2a)	3.830(2)	Sn(1)–C(1)	2.147(3)	Sn(2)–O(1)	2.038(2)
Sn(1)–O(1)	2.076(2)	Sn(1)–C(11)	2.131(3)	Sn(2)–C(3)	2.126(4)
		Sn(2)–F(1)	2.235(2)	Sn(2)–C(21)	2.132(3)
Bond Angles					
O(1)–Sn(1)–F(1)	74.59(8)	F(1)–Sn(1)–C(1)	89.4(1)	F(1)–Sn(2)–C(3)	87.2(1)
O(1a)–Sn(1)–F(1)	150.34(9)	F(1)–Sn(1)–C(11)	91.0(1)	F(1)–Sn(2)–C(21)	88.0(1)
O(1)–Sn(1a)–F(2)	48.08(7)	F(2a)–Sn(1)–C(1)	110.3(1)	F(2)–Sn(2)–C(3)	97.0(1)
O(1)–Sn(1)–F(2a)	117.00(7)	F(2a)–Sn(1)–C(11)	62.0(1)	F(2)–Sn(2)–C(21)	99.6(1)
O(1)–Sn(1)–O(1a)	75.8(1)	C(1)–Sn(1)–C(11)	131.2(2)	C(3)–Sn(2)–C(21)	133.7(2)
O(1)–Sn(1)–C(11)	124.8(1)	O(1)–Sn(2)–F(1)	73.30(8)	Sn(1)–O(1)–Sn(2)	104.5(1)
O(1a)–Sn(1)–C(11)	105.2(1)	O(1)–Sn(2)–F(2)	91.28(9)	Sn(1)–O(1)–Sn(1a)	104.2(1)
O(1a)–Sn(1)–C(1)	97.8(1)	O(1)–Sn(2)–C(3)	101.8(1)	Sn(2)–O(1)–Sn(1a)	141.1(1)
O(1)–Sn(1)–C(1)	102.1(1)	O(1)–Sn(2)–C(21)	120.6(1)	Sn(1)–F(1)–Sn(2)	96.03(8)
F(1)–Sn(1)–F(2a)	152.85(6)	F(1)–Sn(2)–F(2)	164.55(8)		

<sup>a</sup>  $a = -X + 0.5, -Y + 0.5, -Z$ .

These compounds are colorless, crystalline solids which have sharp melting points. They are very soluble in common organic solvents such as chloroform. Their structure in solution follows from  $^{13}\text{C}$  and  $^{119}\text{Sn}$  NMR spectroscopy. Both  $^{119}\text{Sn}$  chemical shifts and  $^1J(\text{Sn}-\text{C})$  couplings are indicative of tetracoordinate tin atoms with a  $\text{C}_2\text{SnO}_2$  substituent pattern.<sup>14</sup> The satellite pattern as well as the satellite-to-signal integral

ratios<sup>4b,15,16</sup> proves unambiguously the connectivity of the carbon, oxygen, and tin atoms in **8–10**. For instance, in **8** and **9**, the  $^2J(\text{Sn}-\text{O}-\text{Sn})$  satellites are twice as intense as the  $^2J(\text{Sn}-\text{C}-\text{C}-\text{Sn})$  and  $^3J(\text{Sn}-\text{C}-\text{C}-\text{Sn})$  satellites, respectively. In **10**, however, there are two  $^2J(\text{Sn}-\text{O}-\text{Sn})$  satellites, and both are of the same integral ratio.

(15) Berwe, H.; Haas, A. *Chem. Ber.* **1987**, *120*, 1175.

(16) Masamune, S.; Sita, L. R. *J. Am. Chem. Soc.* **1985**, *107*, 6390.

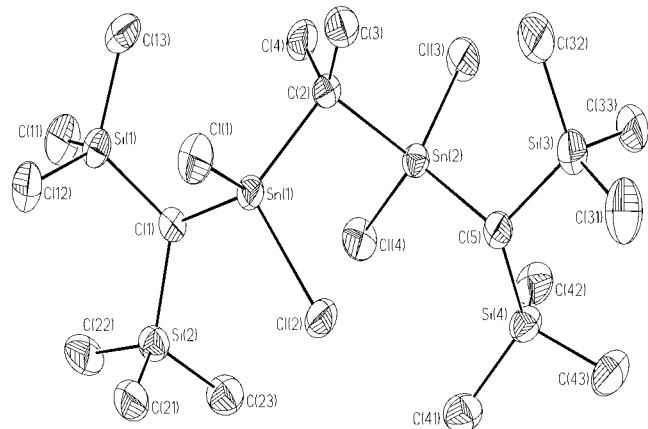


**Figure 1.** General view (SHELXTL-PLUS) of a molecule showing 30% probability displacement ellipsoids and the atom numbering for **3**.

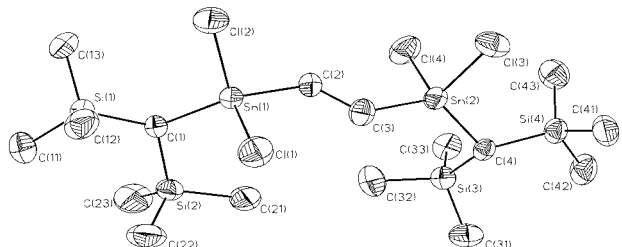
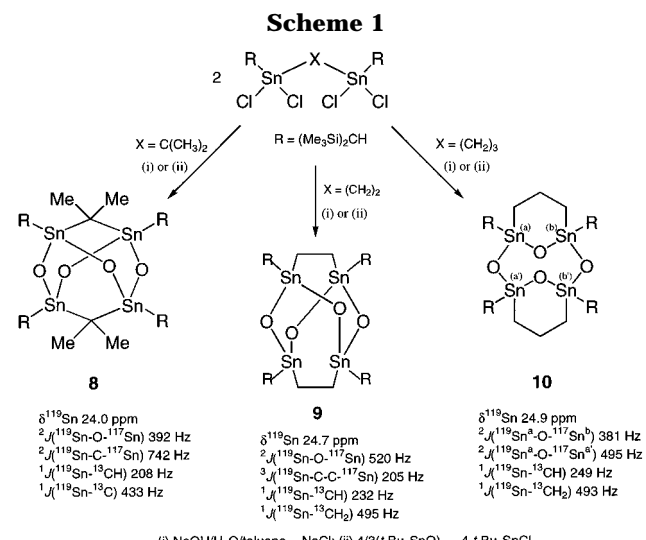


**Figure 2.** General view (SHELXTL-PLUS) of a molecule showing 30% probability displacement ellipsoids and the atom numbering scheme for **6**.



The solution-state structures of **8** and **10** are retained in the solid state, as shown by X-ray crystallography (see below) and also by the  $^{119}Sn$  CP MAS NMR chemical shifts (**8**,  $\delta$  24.4 ppm; **10**,  $\delta$  24.0 ppm,  $^2J^{(119)Sn-O-117Sn} = 436$  Hz,  $\delta$  34.3 ppm,  $^2J^{(119)Sn-O-117Sn} = 436$  Hz), being almost identical with the  $^{119}Sn$  chemical shifts measured in solution. The observation of two equally intense signals in the  $^{119}Sn$  CP MAS spectrum of **10** reflects the nonequivalence of Sn(1) and Sn(2) within one molecule of **10**, as was shown by its crystal structure (see below).

The molecular structures of the organotin oxides **8** and **10** are shown in Figures 3 and 4, respectively.

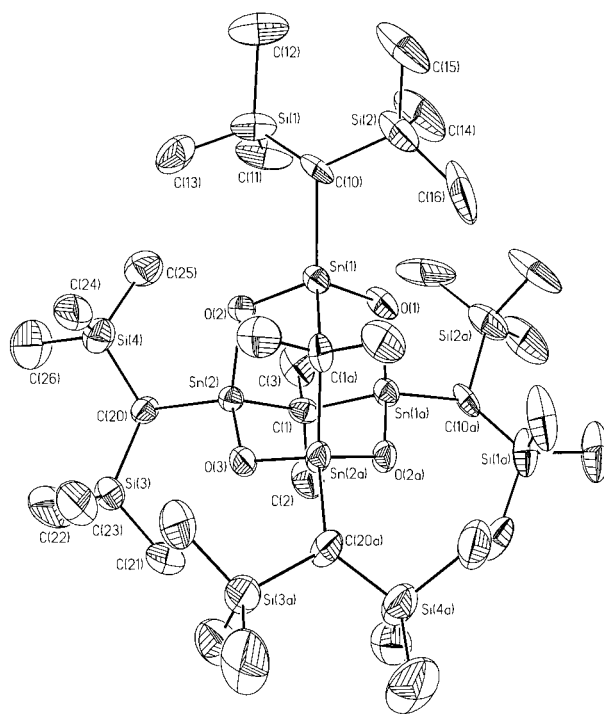


**Figure 3.** General view (SHELXTL-PLUS) of a molecule showing 30% probability displacement ellipsoids and the atom numbering (symmetry transformations used to generate equivalent atoms:  $a = -X, -Y, -Z + 0.5$ ) for **8**.

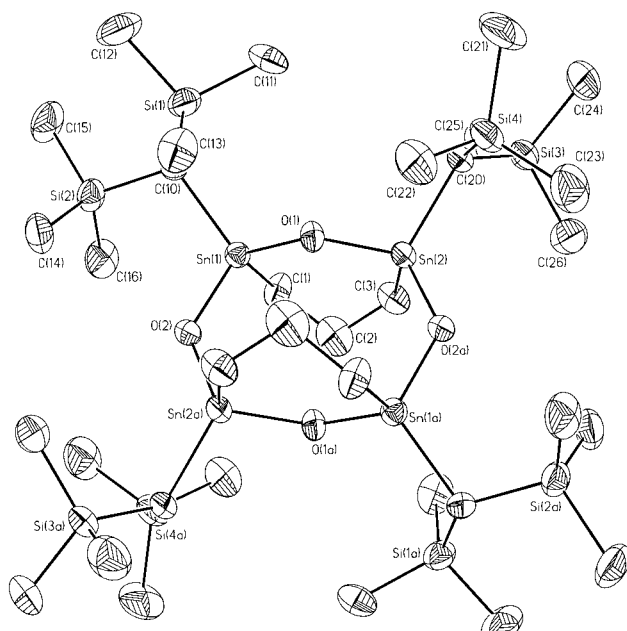


**Figure 4.** General view (SHELXTL-PLUS) of a molecule showing 30% probability displacement ellipsoids and the atom numbering (symmetry transformations used to generate equivalent atoms:  $a = -X, -Y, -Z + 1$ ) for **10**.

Selected bond lengths and bond angles are listed in Table 3. Compound **8** shows an adamantane-type structure with distorted tetrahedral tin atoms. The deviation from the ideal geometry is especially manifested in large Sn–O–Sn ( $121.4(5)$ – $124.0(4)^\circ$ ), C(1)–Sn(2)–C(20) ( $114.4(4)^\circ$ ), and C(1a)–Sn(1)–C(10) ( $118.9(4)^\circ$ ) angles and results from the bulky  $(Me_3Si)_2CH$  and bridging  $CMe_2$  groups.

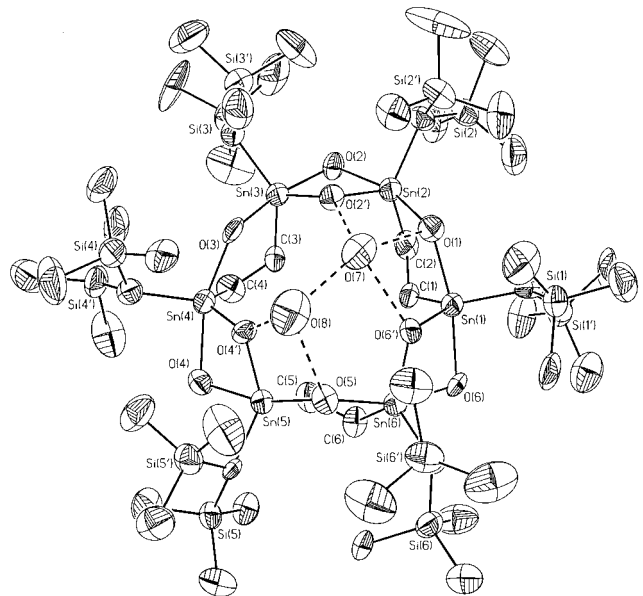


**Figure 5.** General view (SHELXTL-PLUS) of a molecule showing 30% probability displacement ellipsoids and the atom numbering scheme for **9a**.

The structure of **10** is comparable to those of related siloxanes<sup>17</sup> and to  $[\text{Ph}(\text{S})\text{Sn}(\text{CH}_2)_3\text{Sn}(\text{S})\text{Ph}]_2$ .<sup>5</sup> The  $\text{C}_3\text{-OSn}_2$  six-membered rings are mutually trans. The tin atoms are of distorted tetrahedral configuration, with the greatest deviations found for the  $\text{C}(1)\text{-Sn}(1)\text{-C}(10)$  and  $\text{C}(3)\text{-Sn}(2)\text{-C}(20)$  angles of  $119.3(3)$  and  $120.0(3)^\circ$ , respectively. In both **8** and **10**, the  $\text{Sn}\text{-O}$  and  $\text{Sn}\text{-C}$  bond lengths are comparable to those of related diorganotin oxides.<sup>3</sup>

Attempts to grow single crystals of **9** under water-free conditions failed.

**Unexpected Formation of the Hexanuclear Organotinoxo Cluster **9a**.** Compound **9** reacts with air moisture to provide  $\{\text{O}[(\text{RSn}(\text{CH}_2)_2\text{SnR})\text{OH}]\text{OH}\}_3\cdot 2\text{H}_2\text{O}$  (**9a**) as a colorless crystalline solid. The  $^{119}\text{Sn}$  CP MAS NMR spectrum of **9a** displayed two resonances at  $-163.4$  and  $-168.5$  ppm, with an integral ratio of about 1:2. The chemical shifts are in line with pentacoordination at tin. DTA studies of **9a** revealed loss of 5 mole equiv of water between 95 and  $155^\circ\text{C}$ .

The molecular structure of **9a** is shown in Figure 5. Selected bond lengths and bond angles are listed in Table 4. Compound **9a** consists of six tin atoms, which are connected by a combination of dimethylene, oxygen ( $\text{O}(2')$ ,  $\text{O}(4')$ ,  $\text{O}(6')$ ), and hydroxo ( $\text{O}(1)\text{-O}(6)$ ) bridges, resulting in an alternating connection of four- ( $\text{Sn}_2\text{O}_2$ ) and five- ( $\text{Sn}_2\text{C}_2\text{O}$ ) membered rings. Each tin atom has a trigonal bipyramidal configuration with two carbons ( $\text{C}(1)$ ,  $\text{C}(1')$ ;  $\text{C}(2)$ ,  $\text{C}(2')$ ;  $\text{C}(3)$ ,  $\text{C}(3')$ ;  $\text{C}(4)$ ,  $\text{C}(4')$ ;  $\text{C}(5)$ ,  $\text{C}(5')$ ;  $\text{C}(6)$ ,  $\text{C}(6')$ ) and one oxygen ( $\text{O}(2')$ ,  $\text{O}(4')$ ,  $\text{O}(6')$ ) in equatorial and two OH groups ( $\text{O}(1)$ ,  $\text{O}(2)$ ,  $\text{O}(3)$ ,  $\text{O}(4)$ ,  $\text{O}(5)$ ,  $\text{O}(6)$ ) in axial positions. The bond angles about the tin atoms show slight to moderate differences. Thus, the axial  $\text{O}\text{-Sn}\text{-O}$  angles vary between  $160.7(4)$  and  $166.0(4)^\circ$ . The two sets of equatorial  $\text{C}\text{-Sn}\text{-C}$

(17) (a) Gar, T. K.; Buyakov, A. A.; Gusev, A. I.; Los, M. G.; Kisin, A. V.; Mironov, V. F. *Zh. Obshch. Khim.* **1976**, *46*, 837. (b) Dubchak, I. L.; Shklover, V. E.; Timofeeva, T. V.; Struchkov, Yu. T.; Zhdanov, A. A.; Kashutina, E. A.; Shchegolikhina, O. I. *Zh. Strukt. Khim.* **1981**, *22*, 147.

**Scheme 2**

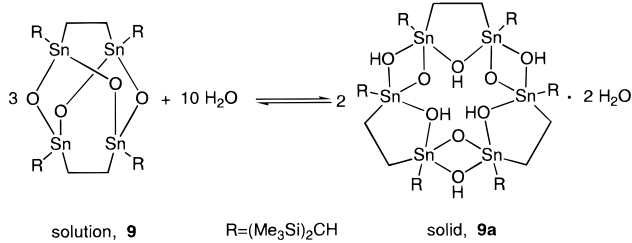
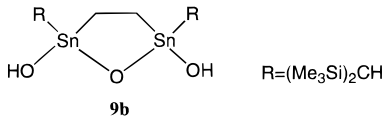
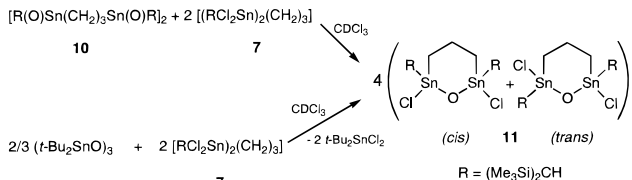


**Chart 2**



**Scheme 3**



angles exhibit values between  $121.4(7)$  and  $128.1(5)^\circ$  as well as  $114.8(5)$  and  $124.5(4)^\circ$ , while the  $\text{C}\text{-Sn}\text{-O}$  angles vary between  $107.4(5)$  and  $122.4(6)^\circ$ .

A stabilizing factor in the structure of **9a** seems to be the two water molecules  $\text{O}(7)$  and  $\text{O}(8)$ , which show strong to moderate hydrogen bridges of  $2.71(2)$ – $2.98(2)$  Å to  $\text{O}(1)$ ,  $\text{O}(2')$ ,  $\text{O}(4')$ ,  $\text{O}(5)$ , and  $\text{O}(6')$  and among each other. The bulky  $(\text{Me}_3\text{Si})_2\text{CH}$  groups show a clockwise orientation and prevent any intermolecular interactions.

Dissolving single crystalline **9a** in  $\text{CDCl}_3$  resulted in reformation of **9** and water, as was evidenced by a single  $^{119}\text{Sn}$  NMR resonance at  $24.7$  ppm, with  $^2J(^{119}\text{Sn}\text{-O}-^{117}\text{Sn})$  and  $^3J(^{119}\text{Sn}\text{-C-C-}^{117}\text{Sn})$  satellites of  $520$  and  $205$  Hz, respectively.

The molecular weight determination also shows that **9a** easily loses water to give **9** in solution. These observations are consistent with the equilibrium shown in Scheme 2.

Such an equilibrium could be achieved by the existence of the monomeric ditin species **9b** (Chart 2).

The existence of monomeric ditin species is strongly implicated in the reaction between **7** and **10**, which yields **11**. Solutions of **11** display two  $^{119}\text{Sn}$  NMR signals at  $86.4$  and  $79.0$  ppm, with an integral ratio of about 14:86. Interestingly, the chemical shifts are near the average of the chemical shifts of  $118.6$  and  $24.9$  ppm found for **10** and **7**, respectively. This indicates that the tin atoms in **11** are tetracoordinate, with a  $\text{C}_2\text{SnCl}_2$  substituent pattern. The molecular mass of **11** (687 g/mol in  $\text{CH}_2\text{Cl}_2$ ) is also consistent with a monomeric ditin species (Scheme 3). We tentatively assign the major  $^{119}\text{Sn}$  signal at  $79.0$  ppm to the trans isomer of **11**.

The monomeric nature of **11** is also supported by electrospray studies. In the positive mode, a cluster was detected at  $m/e 685$  corresponding to  $[\mathbf{11} + \text{H}]^+$ , whereas in the negative mode, clusters were observed at  $m/e 719$  and  $755$  representing  $[\mathbf{11} + \text{Cl}]^-$  and  $[\mathbf{11} + \text{H} + 2\text{Cl}]^-$ , respectively.

Chart 3

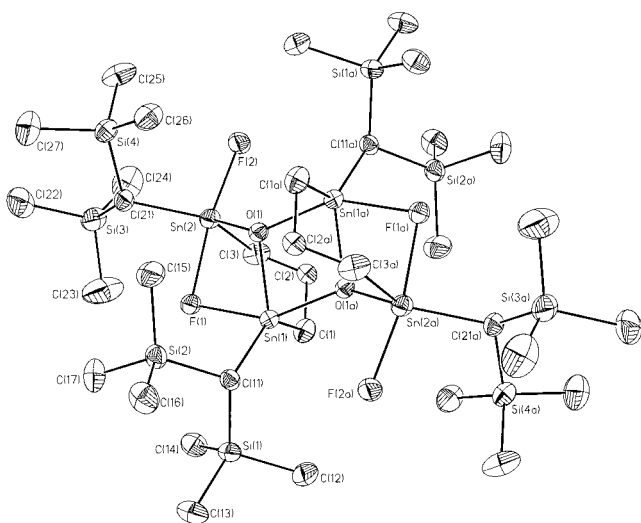
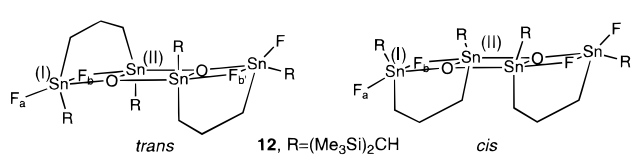
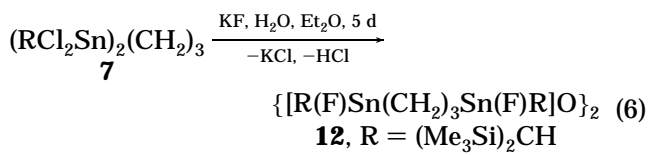


**Figure 6.** General view (SHELXTL-PLUS) of a molecule showing 30% probability displacement ellipsoids and the atom numbering (symmetry transformations used to generate equivalent atoms:  $a = -X + 0.5, -Y + 0.5, -Z$ ) for **12**.

Unfortunately, it was not possible to grow single crystals of **11** suitable for X-ray analysis. However, we were able to exchange chloride by fluoride in order to better characterize these systems.

**Reaction of 7 with KF/H<sub>2</sub>O and Molecular Structure of the Fluorine-Containing Tetraorganodistannoxane 12.** The reaction of **7** with a large excess of potassium fluoride in water/diethyl ether afforded 1,3-bis[bis(trimethylsilyl)methyl]-1,3-difluoro-1,3-distanna-2-oxacyclohexane dimer (**12**) as colorless crystals (eq 6) which have the trans molecular structure in the solid state (see below).



The <sup>19</sup>F and <sup>119</sup>Sn NMR spectra of **12** in CDCl<sub>3</sub> are consistent with the presence in solution of both trans and cis isomers (Chart 3). The ratio of the isomers is approximately 2:1, but the data do not uniquely identify each isomer.

The positive ion ESMS of **12** in acetonitrile/dichloromethane shows the presence of [12 + H]<sup>+</sup> and [12 - F]<sup>+</sup>, confirming that the tetratin units are retained in solution.

The molecular structure of **12** (trans isomer) is shown in Figure 6. Selected bond lengths and bond angles are listed in Table 5. Compound **12** is a centrosymmetric dimer with a center of inversion at (1/4, 1/4, 0). It shows a ladder-type arrangement comparable with those of [(R<sub>2</sub>ClSn)<sub>2</sub>O]<sub>2</sub> (R = alkyl, aryl)<sup>18</sup> and [(tBu<sub>2</sub>FSn)<sub>2</sub>O]<sub>2</sub>,<sup>19</sup> the only other known fluoride-containing tetraorganod-

distannoxanes, with the difference that, as result of the C(1)-C(2)-C(3) bridge, the Sn(2)/Sn(2a) atoms are strongly displaced by  $\pm 0.905(3)$  Å from the F(1)Sn(1)O-(1)Sn(1a)O(1a)F(1a) plane. The planarity of the latter amounts to  $\pm 0.010(1)$  Å. The intramolecular Sn(1)...Sn(2) distance within the four-membered Sn<sub>2</sub>O<sub>2</sub> ring is 3.2536(4) Å.

Each tin atom exhibits a distorted trigonal bipyramidal geometry (geometrical goodness<sup>12b</sup>  $\Delta\sum\vartheta$  79.3° (Sn1), 68.2° (Sn2);  $\Delta\text{Sn}$  (plane) 0.161(2) Å (Sn1), 0.234(2) Å (Sn2)). Sn(1) is coordinated by C(1), C(11), and O(1) in equatorial and by F(1) and O(1a) in axial positions. Sn(2) is coordinated by C(3), C(21), and O(1) in equatorial and by F(1) and F(2) in axial positions. In contrast to [(t-Bu<sub>2</sub>FSn)<sub>2</sub>O]<sub>2</sub>,<sup>19</sup> the Sn(1)-F(1)-Sn(2) bridge in **12** is asymmetric, but the Sn-F distances are of the same order of magnitude as those found for [(Ph<sub>2</sub>XSn)<sub>2</sub>(CH<sub>2</sub>)<sub>n</sub>F]<sup>-</sup>Et<sub>4</sub>N<sup>+</sup> (X = F, Cl, Br, I; n = 1, 2).<sup>9</sup>

The terminal Sn-F distance of 1.993(2) Å is almost identical to the corresponding distance (1.981(7) Å) in [(t-Bu<sub>2</sub>FSn)<sub>2</sub>O]<sub>2</sub><sup>19</sup> and very close to a Sn-F single bond length (1.96 Å).<sup>12a</sup> The Sn(1)...F(2a) distance of 3.830(2) Å is too large to be considered as an interaction. As a consequence of their equatorial and axial positions within the trigonal bipyramidal Sn configuration, the Sn(1)-O(1) (2.076(2) Å) and Sn(2)-O(1) (2.038(2) Å) distances are shorter than the Sn(1)-O(1a) distance of 2.127(2) Å. The Sn-C distances are as expected and comparable to those of related compounds.<sup>3a,b,20</sup>

## Conclusion

It is apparent that both the nature of the spacer linking the ditin precursors and the organo substituent at tin have a profound influence on the hydrolysis/oxygen transfer products. For simple precursors such as RCl<sub>2</sub>Sn(CH<sub>2</sub>)<sub>3</sub>SnCl<sub>2</sub>R, where R is a sterically non-demanding group, the products are double ladders based on tetrameric aggregation of the ditin precursors. Hydrolysis of precursors containing more demanding substituents such as R = (SiMe<sub>3</sub>)<sub>2</sub>CH leads to equilibria between monomeric, dimeric, and trimeric aggregates.

**Acknowledgment.** We are grateful to the Deutsche Forschungsgemeinschaft and the Fonds der Chemischen Industrie for financial support. We thank Mr. Jens Beckmann for recording the <sup>119</sup>Sn MAS spectra. The Dortmunder Gambrinus Foundation is acknowledged for making possible a visit of D.D. at Dortmund University.

**Supporting Information Available:** Tables of all coordinates, anisotropic displacement parameters, and geometric data for **3**, **6**, **8**, **9a**, **10**, and **12** (29 pages). Ordering information is given on any current masthead page.

OM980369L

(18) (a) Alleston, D. L.; Davies, A. G.; Hancock, M.; White, R. F. M. *J. Chem. Soc.* **1963**, 5469. (b) Harrison, P. G.; Begley, M. J.; Molloy, K. C. *J. Organomet. Chem.* **1980**, 186, 213. (c) Graziani, R.; Casellato, U.; Plazzogna, G. *Acta Crystallogr., Sect. C* **1983**, C39, 1188. (d) Puff, H.; Friedrichs, E.; Visel, F. Z. *Anorg. Allg. Chem.* **1981**, 477, 50. (e) Dakternieks, D.; Gable, R.; Hoskins, B. F. *Inorg. Chim. Acta* **1984**, 85, L43. (f) Vollano, J. F.; Day, R. O.; Holmes, R. R. *Organometallics* **1984**, 3, 745. (g) Dakternieks, D.; Jurkschat, K.; van Dreumel, S.; Tiekkink, E. R. T. *Inorg. Chem.* **1997**, 36, 6, 2023.

(19) Beckmann, J.; Biesemans, M.; Hassler, K.; Jurkschat, K.; Martins, J. C.; Schürmann, M.; Willem, R. *Inorg. Chem.*, in press.

(20) Raharinirina, A.; Boese, R.; Schmid, G. *J. Organomet. Chem.* **1990**, 395, 39.